Role of Axial Ligands in the Reactivity of Mn Peroxidase from *Phanerochaete chrysosporium*†

Ross E. Whitwam,‡ Rao S. Koduri,‡,§ Michael Natan,‖,⊥ and Ming Tien*,‡

Department of Biochemistry and Molecular Biology and Department of Chemistry, The Pennsylvania State University, University Park, Pennsylvania 16802

Received October 27, 1998; Revised Manuscript Received May 10, 1999

ABSTRACT: Site-directed mutagenesis was performed on Mn peroxidase (MnP) from the white-rot fungus *Phanerochaete chrysosporium* to investigate the role of the axial ligand hydrogen-bonding network on heme reactivity. D242 is hydrogen bonded to the proximal His of MnP; in other peroxidases, this conserved Asp, in turn, is hydrogen bonded to a Trp. In MnP and other fungal peroxidases, the Trp is replaced by a Phe (F190). Both residues are thought to have a direct influence on the electronic environment of the catalytic center. To study only the active mutants at D242 and F190, we used degenerate oligonucleotides allowing us to screen all 19 possible amino acid mutants at these positions. Two mutants at D242 passed our screen, D242E and D242S. Both mutations impaired only the functioning of compound II. The reactions of the ferric enzyme with H_2O_2 were unaffected by the mutations, as were the reactions of compound I with reducing substrates. The D242S and D242E mutations reduced the first-order rate constant for the reaction of MnP compound II with chelated Mn^{2+} from 233 s^{-1} (wild type) to 154 s^{-1} and 107 s^{-1}, respectively. Three F190 mutants passed our screen, F190V, F190L, and F190W. Similar to mutants at D242, these mutants largely affected the function of compound II. The F190V mutation increased the first-order rate constant for the reduction of compound II by chelated Mn^{2+} to 320 s^{-1}. The F190L mutation decreased this rate to 137 s^{-1}. The F190W mutant was not very stable, but at pH 6.0, this mutation decreased the rate of compound II reduction by Mn^{2+} from 140 s^{-1} in the wild type to 36 s^{-1}. There was no indication that the F190W mutant was capable of forming a protein-centered Trp cation radical. All the mutations altered the midpoint potential of the Fe^{3+}/Fe^{2+} couple of the enzyme, as calculated from cyclic voltammagrams of the proteins. The values were shifted from −96 mV in the wild-type enzyme to −123 mV in D242S, −162 mV in D242E, −82 mV in F190L, −173 mV in F190V, and −51 mV in F190W. Collectively, these results demonstrate that D242 and F190 in MnP influence the electronic environment around the heme and that the reactions of compound II are far more sensitive to this influence than the reduction of compound I.

Lignin is a complex aromatic polymer of phenylpropanoid units, recalcitrant to most forms of microbial attack (*1*). Its degradation is brought about mainly by filamentous fungi, of which the white-rot fungus *Phanerochaete chrysosporium* has been most extensively characterized (*2*−*4*). To degrade lignin, this fungus produces two types of peroxidases, lignin peroxidase (LP)[1] and MnP. The LPs catalyze the one-electron oxidation of nonphenolic aromatic substrates to yield aryl cation radicals (*5*). They also oxidize phenolic substrates to their corresponding radical products (*6*). The MnPs catalyze the oxidation of Mn^{2+} to Mn^{3+} (*7*). Mn^{3+} is a potent oxidant capable of oxidizing a large number of phenolic compounds (*7*). Both fungal peroxidases are potent enzymes oxidizing substrates that other peroxidases are incapable of oxidizing. The Mn^{2+}/Mn^{3+} couple has a midpoint potential of 1.5 V versus NHE (*8*). The reduction potential of LP substrates 1,2-dimethoxybenzene and 1,4-dimethoxybenzene are 1.69 and 1.58 V versus NHE, respectively (*9*).

Despite the unique reactivity, the catalytic cycle of these peroxidases is similar to other peroxidases that experience compound I and compound II intermediate states (*10*−*12*). Furthermore, the active site residues (*13*−*15*) and the three-dimensional structure (*16*−*18*) of both peroxidases are highly homologous to those of other peroxidases. Thus, the structural features which confer unique reactivity to these fungal peroxidases are not obvious. Chemical and biochemical studies indicate that the coordination of hemes by the axial ligand plays a large role in heme reactivity. The axial ligand of cytochrome P450s and chloroperoxidase is a thiolate (*19*, *20*). For catalase, it is a tyrosine (*21*), and for most peroxidases, including MnP and LP, it is a His (*13*, *14*). Although these residues are conserved within each enzyme category, the role of each axial ligand and how it affects the

† This work was supported in part by Department of Energy Grant DE-FG02-87ER13690.

* To whom correspondence should be addressed. Telephone: (814) 863-1165. Fax: (814) 863-8616. E-mail: mxt3@psu.edu.

‡ Department of Biochemistry and Molecular Biology.

§ Present address: Molecular Pharmacology and Biochemistry, Memorial Sloan-Kettering Cancer Center, New York, NY 10021.

‖ Department of Chemistry.

⊥ Present address: Department of Chemistry and Biochemistry, University of Washington, Seattle, WA 98195.

[1] Abbreviations: LP, lignin peroxidase; MnP, Mn peroxidase; DMP, 2,6-dimethoxyphenol; HRP, horseradish peroxidase; CcP, cytochrome *c* peroxidase.

10.1021/bi982568e CCC: $18.00 © 1999 American Chemical Society
Published on Web 06/17/1999

chemistry of the reaction are not well understood.

In this study, we have investigated the role of the axial ligands of MnP reactivity by site-directed mutagenesis. Like other heme peroxidases, the proximal His of MnP is H-bonded to a critical Asp residue (*17*, *22*−*26*). In CcP, the Asp residue is H-bonded to a Trp (*24*). In contrast, a Phe is found in MnP and LP (*17*, *18*). The axial H-bonding network is thought to keep the His imidazole partially deprotonated. This in turn allows the imidazole group to stabilize the heme iron as it cycles through Fe^{3+} and Fe^{4+} states during the peroxidase catalytic cycle (*24*, *27*). Using a modified form of scanning mutagenesis, we have mutated D242 and F190 of MnP to every other possible amino acid and screened the resultant mutants for activity. We only found two active mutants at the D242 site, D242E and D242S. At F190, we found three active mutants, F190L, F190V, and F190W. We performed extensive kinetic characterization of these mutants and show that axial ligands have their strongest influence on the reactions of the compound II state of the enzyme and little if any effect on the reactivity of compound I. These results were predicted by the theoretical studies of Du and Loew (*28*).

MATERIALS AND METHODS

Chemicals. Hydrogen peroxide was purchased from Fisher Scientific. Oxidized glutathione, ampicillin, chloramphenicol, $CaCl_2$, phenylmethanesulfonyl fluoride, Pharmalytes, and oxalic acid were purchased from Sigma Chemical Co. Ultrodex was purchased from Pharmacia. IPTG was purchased from Promega Biotech. The concentration of H_2O_2 was determined spectrophotometrically at 240 nm using an extinction coefficient of 39.4 M^{-1} cm^{-1} (*29*).

Expression and Refolding of MnPs. All the MnPs used in this study were recombinant enzymes, expressed in *Escherichia coli* as previously described (*30*) using the pET21aH4-looped(+) vector and *E. coli* strain BL21(DE3)pLysS (Novagen, Madison, WI). Recombinant MnPs were refolded to active holoenzyme as described previously (*30*).

Mutagenesis of the D242 Site of MnP. The procedure of Kunkel et al. (*31*) was used for oligonucleotide-directed mutagenesis of the pET21aH4looped(+) expression vector. CJ236 was the dut$^-$ung$^-$ strain of *E. coli* used for expression. We developed a screen that would allow us to rapidly identify all the mutants of D242 which are active. First, the Q240 site, two codons away from D242 in MnP, was mutated to a stop codon. The oligonucleotide 5′-GTCGGACTACAGCGCAT-3′ (the site of the mutation is underlined) was used to alter the CAG codon of Q240 to a TAG amber codon. After expression in *E. coli*, the resultant truncated protein was no longer active and could be easily distinguished from wild-type MnP on SDS−PAGE and Western blot analyses due to its smaller size. This truncated clone was used for the subsequent rounds of mutagenesis. It provides a negative background from which any active mutant could be easily identified. These subsequent rounds utilized oligonucleotides that contained two mutations (relative to the truncated clone). The first reintroduced the Q240, eliminating the stop codon, and the second generated the 19 possible mutants at D242. This procedure, screening against a negative background, ensured that any active mutant would not be the wild type making it through the mutagenesis procedure. Four pools of oligonucleotides were designed to reintroduce the Q240 codon back into the truncated mutants of MnP and to alter the D242 site to every other amino acid. Oligonucleotide pool 1 consisted of eight different codons and five different amino acids at the D242 site (Figure 1). Oligonucleotide pool 2 consisted of eight different codons encoding five different amino acids at the D242 site. Oligonucleotide pool 3 consisted of four different codons encoding four different amino acids at the D242 site. Oligonucleotide pool 4 consisted of eight different codons encoding seven different amino acids at the D242 site. After mutagenesis, individual clones were expressed in *E. coli* and the resulting MnPs were subjected to SDS−PAGE and visualized by Western transfer.

Pool 1 5′-GAGCGCAAA(**A/C**)(**T/G/C/T**)**A**GGACTGCAGGCGCAT-3′.
Pool 2 5′-GAGCGCAAA(**A/T**)(**T/G/C/T**)**G**GGACTGCAGGCGCAT-3′
Pool 3 5′-GAGCGCAAA**T**(**T/G/C/T**)CGGACTGCAGGCGCAT-3′
Pool 4 5′-GAGCGCAAA(**A/C**)(**T/G/C/T**)**T** GGACTGCAGGCGCAT-3′
Pool 5 5′-CCATCGATGCTGCGCCC(**A/T/C/G**)**T**(**A/G**)GACTCGACACCC-3′
Pool 6 5′-CCATCGATGCTGCGCCC(**A/T/C/G**)(**A/C/G**)(**A/T/G/C**)GACTCGACACCC-3′

FIGURE 1: Oligonucleotides used for random mutagenesis. Pools 1−4 were used for mutagenesis of D242. Pools 5 and 6 were used for F190. The sites of the mutation which mutated the amber codon in the truncated MnP back to either Q240 or S192 are underlined. The sites of the partial degeneracy which represented different non-aspartate or non-phenylalanine codons are shown in bold.

Mutagenesis of the F190 Site of MnP. The procedure for mutating F190 was similar to that of D242 described above. Again, a TAG codon was generated, this time at Ser 192. This amber codon was removed from subsequent mutagenesis. Two oligonucleotide pools were used. Oligonuclotide pool 5 consisted of four different amino acids, and pool 6 consisted of the remaining 15 possible amino acids as shown in Figure 1. From the screening procedure, F190L, F190V, and F190W were obtained as the only active mutants.

Preparation of Recombinant MnPs. A modification of the previously described scheme (*30*) was used to purify the recombinant MnPs. Refolded preparations of recombinant MnP were dialyzed exhaustively against 50 mM sodium Tris-HCl (pH 8.0) at 4 °C. Upon dialysis, a precipitate formed. The dialyzed sample was centrifuged at 10000*g* for 15 min at 4 °C, and the supernatant was loaded onto a DEAE-BioGel A column (1.5 cm × 20 cm) in 50 mM Tris-HCl (pH 8.0). The enzyme was eluted with 300 mL of a linear gradient of 0 to 0.15 M $CaCl_2$ in the column buffer. Fractions exhibiting the highest specific activity were pooled and dialyzed against H_2O. This preparation was then further purified by preparative flat-bed isoelectric focusing. Isoelectric focusing was performed with a Pharmacia/LKB Multiphor II apparatus (Pharmacia, Piscataway, NJ). Gels were made of Ultrodex, and a pH 4.2 to 8.0 gradient was established using Pharmalytes. After isoelectric focusing, the enzyme was dialyzed against H_2O and stored until it was assayed. The MnP preparations typically exhibited Rz values (ratio of 407 nm to 280 nm absorbances) in the range of 3−4, characteristic of highly purified MnP (*10*). The MnP concentrations were quantitated spectrophotometrically at 407 nm using an extinction coefficient of 127 mM^{-1} for MnP isozyme H4 (*32*).

Steady-State Methods. For the D242 mutants, the determinations of k_{cat}, $K_m(H_2O_2)$, and $K_m(Mn^{2+}/oxalate)$ were performed in 0.5 mM sodium oxalate and 10 mM sodium succinate (pH 4.5) at 28 °C. The oxidation of Mn^{2+} to Mn^{3+} was monitored at 270 nm using an extinction coefficient of 5.5 mM^{-1} (*11*). For the F190 mutants, steady-state experi-

ments were performed with Mn^{2+}−malonate complexes with 50 mM sodium malonate (pH 4.5) at 28 °C. Malonate was used as a chelator because of the high K_m for Mn^{2+} exhibited by some of these mutants (in contrast to the D242 mutants). A higher concentration of oxalate would have been required to form complexes with the higher concentrations of Mn^{2+}. This would have resulted in the formation of the 2:1 oxalate−Mn^{2+} complex. This complex is not oxidized by MnP (*11*). The higher concentration of malonate used to complex the higher Mn^{2+} concentration still resulted in the formation of the 1:1 complex (*11*). The oxidation of Mn^{2+} to Mn^{3+} was monitored at 270 nm using an extinction coefficient of 8.5 mM^{-1} (*11*).

Approximately 10−20 nM enzyme was used for steady-state determinations. The K_m for H_2O_2 was determined with incubations containing 0.2 mM $MnSO_4$. The K_m for Mn^{2+}−oxalate and the K_m for Mn^{2+}−malonate were determined with incubations containing 50 μM H_2O_2. Due to H_2O_2 inhibition of the enzymes, the initial velocity data were analyzed according to the method of Cleland (*33*), as discussed previously (*30*). All studies were carried out at 28 °C.

Transient-State Methods. The stopped-flow apparatus was purchased from KinTek Instruments (State College, PA) and contained a 2.6 cm light path. Rates were determined from kinetic traces that were composed of the average of three shots. All reactions were carried out at 28 °C. The rate of compound I formation from the reaction of ferric enzyme with H_2O_2 was monitored at 397 nm, the isosbestic wavelength between compound I and compound II (*11*). The rate of compound I formation was studied with varying concentrations of H_2O_2 and 0.7−1.0 μM recombinant MnP in 20 mM sodium tartrate (pH 4.5).

Reactions of compound I and compound II with Mn^{2+} and DMP were studied under single-turnover pseudo-first-order conditions with the stopped-flow apparatus in the double-mixing, three-syringe mode. The stopped-flow apparatus is designed with a stepper motor and without a stopping syringe to allow for these double-mixing experiments as previously described (*11*). Briefly, to generate compound I, ferric enzyme is mixed with 1 equiv of H_2O_2. The solution is then aged in the delay line for 1.5 s to allow for complete formation of compound I. The second push from the stepper motor forced the mixing of the resultant compound I with the contents of the third syringe that contained the reducing substrate (Mn^{2+} or DMP).

Reduction of compound I to compound II by Mn^{2+} was monitored at 417 nm, the isosbestic wavelength between resting ferric enzyme and compound II. Typically, 1 μM enzyme was used with varying Mn^{2+} concentrations in 20 mM sodium tartrate at either pH 2.5 or 4.5, as indicated in the Results.

The reduction of compound II by Mn^{2+}−oxalate or by Mn^{2+}−malonate was monitored at 426 nm, the isosbestic wavelength between the resting ferric enzyme and compound I. Typically, 1 μM enzyme was used with varying Mn^{2+} concentrations in either 0.5 mM sodium oxalate, 10 mM sodium succinate (pH 4.5), or 50 mM sodium malonate (pH 4.5).

Difference Spectra of the Reaction of Ferric Enzyme with H_2O_2. Difference spectra were constructed for wild-type MnP and the F190W mutant in 20 mM MES (pH 6.0). Equimolar concentrations of MnP and H_2O_2 were allowed to react in the stopped-flow apparatus under single-shot conditions. The total absorbance change at each wavelength was determined by allowing the reaction to run to completion (more than seven half-lives).

Cyclic Voltammetry. Electrochemical determinations were carried out on a PAR model 273A potentiostat/galvanostat operated using the model 270 software on a Gateway 486 IBM-compatible computer. Approximately 3−4 mL of 15−40 μM enzyme in 100 mM sodium sulfate and 40 mM potassium phosphate (pH 7.0) was placed in an anaerobic spectrochemical cuvette, with airtight ports for a carbon working electrode, a platinum wire counter electrode, and an Ag/AgCl reference electrode. The carbon electrode was polished with 0.05 μM diamond paste prior to each use. The anaerobic cuvette contained a stopcock, and the enzyme solutions were made anaerobic by alternating regimens of vacuum evacuation and purging with oxygen-free argon gas. At scan rates slower than 1000 mV/s, the charge transfer to MnP was irreversible. The Fe^{3+}/Fe^{2+} couple of the heme group could be reduced, but could not be reoxidized. As faster scan rates and higher enzyme concentrations were used, the charge transfer becomes quasi-reversible. The cyclic voltammogram (CV) of each enzyme solution was obtained by subtracting the CV of the electrolyte solution from the CV of the electrolyte/enzyme solution. The midpoint potential ($E°'$) was calculated as described by Bard and Faulkner (*34*). To obtain an $E°'$ with respect to NHE, 197 mV was subtracted.

RESULTS

Screening for Active Mutants of MnP. To characterize only active mutants, we performed a modified form of scanning mutagenesis. Using degenerate oligonucleotides, we were able to screen, on the basis of statistical considerations, all possible mutants at the D242 position of MnP. Mutagenesis was performed on a truncated clone with a stop codon introduced at Q240. Thus, we started with a negative (no activity) background. Subsequent mutagenesis at D242 was performed with degenerate oligonucleotides that mutated both D242 (to all 19 possible mutants) and the stop codon back to Q240. Clones which yielded successfully mutated MnP at D242 were easily identified because they had been concomitantly returned to their full wild-type size (37 vs 24 kDa); any clones in which the introduced stop codon was successfully mutated back to Q240 would concomitantly be mutated at the D242 site. The mutant MnPs from 24 such clones from the oligonucleotide pool 1 (see Materials and Methods) were refolded under the conditions which yielded active wild-type enzyme, as were 24 clones from oligonucleotide pool 2, 12 clones from oligonucleotide pool 3, and 24 clones from oligonucleotide pool 4. All 84 preparations were assayed for MnP activity in microtiter wells. Of these, only four exhibited detectable activity. These four clones were sequenced, revealing two that contained D242S mutations and two that contained D242S mutations. A D242E clone and a D242S clone were used to produce large-scale quantities of the mutant MnPs.

A similar screening procedure for F190 yielded F190L, F190V, and F190W as the only active mutants.

Enzyme Stability. The F190W mutant differed from the wild-type enzyme and the other mutant enzymes. The

Table 1: Steady-State Kinetic Parameters of Wild-Type MnP and D242 Mutants of MnP[a]

enzyme	$K_m(H_2O_2)$ (μM)	$K_m(Mn^{2+})$ (μM)	k_{cat} (s^{-1})	$k_{cat}/K_m(H_2O_2)$ (M^{-1} s^{-1})	$k_{cat}/K_m(Mn^{2+})$ (M^{-1} s^{-1})
wild-type	96	56	450	4.7×10^6	8.0×10^6
D242S	54	82	250	4.6×10^6	3.0×10^6
D242E	35	44	72	2.1×10^6	1.6×10^6

[a] All enzymes were expressed in *E. coli* as described in Materials and Methods. Assays were performed at pH 4.5 as described in Materials and Methods. The initial velocity data were analyzed according to the method of Cleland (*33*).

concentrated F190W enzyme was not stable at pH ≤6.0. In contrast, the wild-type enzyme and the other mutants at D242 and F190 were all stable at pH values as low as 2.5 (data not shown). The instability of the F190W mutant suggests that this mutation may have introduced structural perturbations that did not occur with the F190L or F190V mutations.

Steady-State Analyses of D242 Mutants. The steady-state kinetic constants for the D242 mutants of MnP are listed in Table 1. Experiments with the D242 mutants of MnP did not require elevated Mn^{2+} concentrations and were performed in oxalate/succinate buffer to be consistent with earlier studies (*11*). The K_m for H_2O_2 was decreased for both mutants, whereas the K_m for Mn^{2+}, within experimental error, was not altered. K_m, however, is the ratio of the two independent fundamental constants revealed by steady-state kinetics: k_{cat} and k_{cat}/K_m. Changes in the Michaelis constant, K_m, of an enzyme simply reflect changes occurring independently in the k_{cat} and k_{cat}/K_m values of that enzyme. In this regard, D242S and D242E both exhibited a decrease in k_{cat}. The D242S mutation reduced the k_{cat} of MnP to 250 s^{-1}, approximately half of that of the wild-type enzyme, whereas the D242E mutation reduced the k_{cat} approximately 6-fold to 73 s^{-1}. Little or no change was observed for either mutant in k_{cat}/K_m for H_2O_2 which is consistent with the mutations not affecting the reactivity of the enzyme toward H_2O_2. However, a decrease in k_{cat}/K_m was observed for Mn^{2+}, indicating that the reactivity of the enzyme toward Mn^{2+} had been compromised.

Steady-State Analyses of F190 Mutants. At the low enzyme concentrations that were used for steady-state kinetic analyses (10−20 nm), the F190W mutant was stable at pH 4.5, the pH optimum of the wild-type enzyme, permitting initial velocity studies. This suggests that protein−protein interactions caused the instability observed at high enzyme concentrations. The experimental conditions are different from those used for the D242 mutants. Initial experiments indicated that the K_m for Mn^{2+} was dramatically increased with this mutant such that the Mn^{2+} concentration required to saturate the enzyme was much higher than the oxalate concentration used as the chelator. If oxalate was used at concentrations found physiologically (*11*), the 1:1 Mn^{2+}−oxalate complex would not be formed. Therefore, these experiments were performed with malonate as the Mn^{2+} chelator rather than the physiologically relevant oxalate (*11*, *35*).

The steady-state kinetic constants for the F190 mutants are shown in Table 2. The k_{cat} values of the F190L and F190W mutants were decreased, whereas for the F190V mutant, an increase in k_{cat} was observed (Table 2). As with the mutations at D242, no changes were observed with k_{cat}/K_m for H_2O_2 with the mutants, but the k_{cat}/K_m was slightly decreased for Mn^{2+}. As mentioned above, the $K_m(Mn^{2+})$ of the F190W mutant exhibits a more marked decrease, much more than those observed with other mutants. It is 30-fold higher than the wild-type value.

Table 2: Steady-State Kinetic Parameters of Wild-Type MnP and F190 Mutants of MnP[a]

enzyme	K_m (H_2O_2) (μM)	K_m (Mn^{2+}) (μM)	k_{cat} (s^{-1})	k_{cat}/K_m (H_2O_2) (M^{-1} s^{-1})	k_{cat}/K_m (Mn^{2+}) (M^{-1} s^{-1})
wild-type	147	33 (71)	508 (260)	3.5×10^6	1.4×10^7 (3.2×10^7)
F190L	73	38	314	4.3×10^6	8.0×10^6
F190V	205	81	683	3.3×10^6	8.0×10^6
F190W	36	1010 (2200)	56 (47)	2.0×10^6	5.5×10^4 (2.1×10^4)

[a] All enzymes were expressed in *E. coli* as described in Materials and Methods. Assays were performed at pH 4.5 or 6.0 (value in parentheses) as described in Materials and Methods. The initial velocity data were analyzed according to the method of Cleland (*33*).

Table 3: Pre-Steady-State Kinetic Parameters of Wild-Type MnP and D242 Mutants of MnP at pH 4.5 (Ferric Enzyme and Compound II) and pH 2.5 (Compound I)[a]

	$k \times 10^{-6}$ (M^{-1} s^{-1})	$k \times 10^{-4}$ (M^{-1} s^{-1})		K_d (μM)	k (s^{-1})
enzyme	ferric with H_2O_2	cpd I with Mn^{2+}	cpd I with DMP	cpd II with Mn^{2+}−oxalate	cpd II with Mn^{2+}−oxalate
wild-type	4.0	4.2	2.5	13	233
D242S	3.5	7.9	2.3	10	153
D242E	3.9	5.0	2.0	13	137

[a] All enzymes were expressed in *E. coli* as described in Materials and Methods. Assays were performed at pH 4.5 as described in Materials and Methods.

Steady-state studies were also performed at pH 6.0 with the F190W mutant. At this higher pH, concentrated samples of the F190W mutant, required for pre-steady-state studies, did not precipitate. Thus, the steady-state experiments were performed for comparative purposes. At this higher pH, in 20 mM MES (pH 6.0), similar results were obtained. The K_m for Mn^{2+} of the mutant was increased, and the k_{cat} was decreased (Table 2, values in parentheses).

Pre-Steady-State Analysis of the D242 Mutants. The pre-steady-state rate constants for wild-type and D242 mutants of MnP are listed in Table 3. The rate of compound I formation is not affected by any of the mutations. This is consistent with the $k_{cat}/K_m(H_2O_2)$ values obtained in the steady-state determinations, which did not significantly differ from the wild-type values. The reaction between Mn^{2+} and compound I of wild-type MnP is too fast at pH 4.5 to measure in the stopped-flow spectrophotometer. Given the dead time of our instrumentation and the extinction coefficient of MnP, the rate constant for this reaction is estimated to be $>10^7$ M^{-1} s^{-1} at pH 4.5. At pH 2.5, the reaction is slower and measurable. For the wild-type MnP, the rate constant is 4.2×10^4 M^{-1} s^{-1}. The mutation to Ser or to Glu at Ser242 had little or no effect on the reactivity of compound I toward Mn^{2+}. The rates were actually increased by the D242S mutation.

The reduction of MnP compound II to the resting ferric enzyme requires chelated Mn^{2+} and involves a rapid equilibrium binding step between compound II and the Mn^{2+}−chelator complex (*11*). The dissociation constant, K_d, between compound II and Mn^{2+} and the first-order rate constant, k,

Table 4: Pre-Steady-State Kinetic Parameters of Wild-Type MnP and F190 Mutants of MnP at pH 4.5 (Ferric Enzyme and Compound II) and pH 2.5 (Compound I)[a]

	$k \times 10^{-6}$ (M^{-1} s^{-1})	$k \times 10^{-4}$ (M^{-1} s^{-1})		K_d (μM)	k (s^{-1})
enzyme	ferric with H_2O_2	cpd I with Mn^{2+}	cpd I with DMP	cpd II with Mn^{2+}−malonate	cpd II with Mn^{2+}−malonate
wild-type	4.0	4.2	2.5	20	225
F190L	5.4	10	2.1	17	137
F190V	4.1	3.3	2.4	56	320

[a] All enzymes were expressed in *E. coli* as described in Materials and Methods. Assays were performed as described in Materials and Methods.

for the conversion of compound II to the resting MnP were determined by fitting data to the equation $k_{obs} = k/(1 + K_d/[Mn^{2+}])$. Similar to the steady-state experiments described above, the reactions of compound II of the D242 mutants were studied with Mn^{2+}−oxalate. The mutation had no effect on the K_d values for Mn^{2+}−oxalate. The values varied from 10 to 13 μM (Table 3). The mutations, however, did cause a decrease in the first-order rate constants. Both mutations caused a near 2-fold decrease in the rate.

Pre-Steady-State Analysis of the F190 Mutants. Similar to the D242 mutants, single-turnover experiments were performed at pH 4.5 and 2.5. However, for the F190W mutants, experiments were also performed at pH 6.0 due to problems associated with protein aggregation. The results obtained with the F190L and F190V mutants are shown in Table 4. Similar to results obtained with the D242 mutants, reactions of the ferric enzyme with H_2O_2 were not affected by the mutations at F190.

Reactions of compounds I and II with Mn^{2+} were studied with malonate rather than oxalate as a chelator, similar to conditions used for steady-state kinetics. In reactions with compound I, the F190L mutation increased the rate constant slightly over 2-fold, whereas the F190V mutation resulted in a 20% decrease in the rate constant. The changes in the rate constants with compound II and Mn^{2+} were greater than those observed with compound I for both of these mutant enzymes. Although the K_d for Mn^{2+} was not greatly altered, the first-order rate constant was reduced to 60% of its value by the F190L mutation. In contrast, the F190V mutant slightly increased the first-order rate constant. This is in accord with the results of the steady-state analysis (Table 2).

As mentioned above, all pre-steady-state analyses for the F190W mutant were performed at pH 6.0. The rate constants from these analyses for both wild-type MnP and the F190W mutant at pH 6.0 are shown in Table 5. Consistent with steady-state results, the reaction with H_2O_2 was not altered by the F190W mutation. The value of 6×10^6 M^{-1} s^{-1} determined for the mutant is within experimental error of the value of 4×10^6 M^{-1} s^{-1} determined for the wild-type enzyme.

For reactions of compound I with Mn^{2+}, the rate were too fast even at pH 6.0 or 8.5. Likewise, the reduction of compound I of the F190W mutant by free Mn^{2+} was also too fast at these two pH values.

Reactions of compound II at pH 6.0 in 20 mM MES buffer utilized MES as the chelator. Mn^{2+}−MES was able to support the reduction of MnP compound II. At pH 6.0, the

Table 5: Pre-Steady-State Kinetic Parameters of Wild-Type MnP and F190W MnP at pH 6.0[a]

	$k \times 10^{-6}$ (M^{-1} s^{-1})	$k \times 10^{-4}$ (M^{-1} s^{-1})		K_d (μM)	k (s^{-1})
enzyme	ferric with H_2O_2	cpd I with Mn^{2+}	cpd I with DMP	cpd II with Mn^{2+}−MES	cpd II with Mn^{2+}−MES
wild-type	3.7	>10000	2.3	20	140
F190W	5.7	>10000	2.4	15	36

[a] All enzymes were expressed in *E. coli* as described in Materials and Methods. Due to the instability of the F190W mutant at pH 4.5, assays were performed at pH 6.0 as described in Materials and Methods.

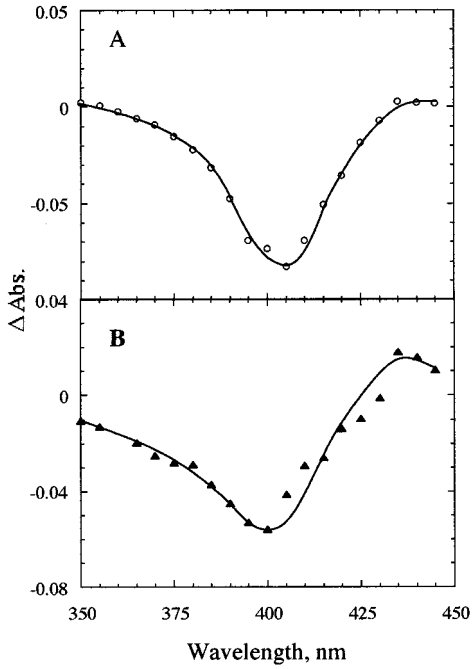

FIGURE 2: Difference spectra of species formed from the reaction of ferric enzyme with H_2O_2. Either the F190W mutant (A) or the wild-type (B) enzyme (1 μM) in 20 mM MES (pH 6.0) (final) was mixed with an equal concentration of H_2O_2, and the resulting difference in absorbance (obtained after seven half-lives) is plotted as a function of wavelength.

K_d of wild-type MnP compound II for chelated Mn^{2+} is still 20 μM, the same value determined at pH 4.5. However, the first-order rate constant for the reduction was reduced to 140 s^{-1}. At pH 6.0, the K_d for Mn^{2+} of compound II of the F190W mutant is 15 μM, largely unchanged from that of wild-type MnP. The first-order rate constant for the reduction of F190W compound II by Mn^{2+} at pH 6.0 is reduced to 36 s^{-1}.

Compound I of F190W. To investigate whether the nature of compound I in the F190W mutant of MnP was altered as a consequence of the mutation, a difference spectrum was obtained from the reaction of ferric MnP F190W with 1 equiv of H_2O_2. The resulting spectrum (Figure 2A) is largely the same as that of the wild-type enzyme (Figure 2B), with the trough at 405 nm characteristic of wild-type compound I formation. It is lacking a major peak at 420 nm expected from the formation of a compound II-like intermediate without a porphyrin-based delocalized π-cation radical.

Electrochemistry. The midpoint potentials of the Fe^{3+}/Fe^{2+} couple of the D242 and F190 mutants of MnP were determined by cyclic voltammetry at pH 7.0. The CVs, shown in Figure 3, were determined on carbon electrodes

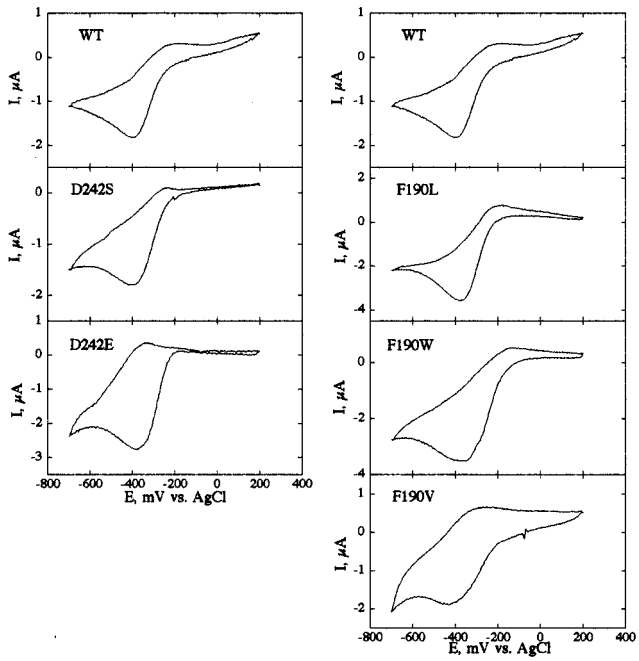

FIGURE 3: CVs of wild-type MnP and its mutants. CVs were recorded at 1000 mV/s. CVs correspond to the enzyme as marked in the panel. CVs were recorded at pH 7.0 as described in Materials and Methods.

Table 6: Midpoint Potentials of the Fe^{3+}/Fe^{2+} Couple at pH 7.0 ($E^{\circ\prime}$) of Wild-Type and Mutant MnPs

enzyme[a]	$E^{\circ\prime}$ (mV)[b]	enzyme[a]	$E^{\circ\prime}$ (mV)[b]	enzyme[a]	$E^{\circ\prime}$ (mV)[b]
wild-type	−96	D242E	−162	F190V	−173
D242S	−123	F190L	−82	F190W	−51

[a] All enzymes were expressed in *E. coli* as described in Materials and Methods. [b] Cyclic voltammetry was performed in 100 mM sodium sulfate and 40 mM potassium phosphate (pH 7.0) using a carbon working electrode and an Ag/AgCl reference electrode. All $E^{\circ\prime}$ values are given with respect to the NHE to facilitate comparisons with earlier work.

using an Ag/AgCl reference electrode. The midpoint potentials were calculated by the method of Bard and Faulkner (*34*), in which the midpoint potential between the anodic and cathodic peaks is calculated to be the midpoint potential of the couple being studied. When corrected for the difference between Ag/AgCl and standard hydrogen electrodes, wild-type recombinant MnP gave an $E^{\circ\prime}$ of −96 mV vs NHE. The midpoint potentials of the D242 mutants and the F190 mutants of MnP are shown in Table 6. Using this method, all the mutations altered the midpoint potential of the Fe^{3+}/Fe^{2+} couple of MnP. The F190L and F190W mutations both increased the midpoint potential of MnP, to −82 mV for the F190L mutant and to −51 mV for the F190W mutant. The F190V mutation decreased the midpoint potential of the enzyme to −173 mV. The D242S and D242E mutations both decreased the midpoint potential of the enzyme, to −123 and −162 mV, respectively. However, an examination of the CVs of these mutants (Figure 3) reveals that, while the cathodic and anodic peaks of the CV were shifted about equally from the wild type in all the F190 mutations, in the D242 mutants, only the cathodic peaks was largely shifted relative to the wild-type peaks. The anodic peaks were largely unchanged. Under the conditions that were used, the charge transfer to MnP was only quasi-reversible, with reduction of the Fe^{3+}/Fe^{2+} couple occurring much more readily than its reoxidation, and the comparatively large shift to the cathodic peaks in the D242S and D242E mutants might not so accurately reflect the shift in the midpoint potentials of these mutants.

DISCUSSION

Heme coordination is widely accepted to play a major role in the reactivity of heme proteins. The axial ligand is the Tyr oxygen for catalase, the Cys sulfur for cytochrome P450 and chloroperoxidase, and the His nitrogen for globins and heme peroxidases. However, within a heme protein family such as the peroxidases, differences in reactivity cannot be attributed to the differences in the axial ligand. Closer examination reveals that the hydrogen bonding network of the axial ligands differ in the peroxidases. All heme peroxidases characterized to date have an Asp hydrogen bonded to the axial His. In contrast to CcP, where the Asp is further hydrogen bonded to a Trp, the Trp is replaced by a Phe in LP and MnP.

The purpose of this study was to determine the structural aspects that confer the fungal peroxidases with their greater reactivity. Thus, we mutated the axial ligands of MnP that, in CcP, are hydrogen bonded to the axial His (*24*). At Asp 242, we screen 84 different clones and found four active D242 mutants that represented only two mutations, D242S and D242E. The purpose of the screen was not to find all of the possible active mutants but to maximize our chance of finding active mutants; this we have accomplished. Similar arguments apply for the methodology for the F190 mutants. The results of Kishi et al. (*36*), discussed further below, would argue that we have not identified all possible active mutants, at least at the F190 position.

Our results show that with the exception of F190V, all of the mutations decreased the reactivity of MnP. The k_{cat} of the F190V mutant was 1.34 times greater than that of the wild-type enzyme. This increase was also observed in the transient-state kinetic studies where the reactivity of compound II, the rate-limiting step in steady-state turnover (*11*), was increased in the F190V mutant. The other mutations, at D242 and F190, did cause a decrease in enzyme activity. A corresponding decrease in the K_m of H_2O_2 was also observed. However, this decrease does not reflect a decrease in the affinity of the enzyme for H_2O_2 since the k_{cat}/K_m for H_2O_2 remained unchanged in all of the mutants. The lack of a change in reactivity toward H_2O_2 was also observed in the transient-state kinetic studies. None of the mutations resulted in a significant change in the second-order rate constant between H_2O_2 and ferric enzyme forming compound I. All of the mutations did alter the reactivity of the enzyme toward chelated Mn^{2+}. In steady-state kinetics, with the exception of the F190W mutant, no change was observed in the K_m for Mn^{2+}. With the corresponding change in k_{cat}, this results in a decrease in k_{cat}/K_m for Mn^{2+} for all of these mutants. The transient-state kinetic results again corroborated the steady-state results. In contrast to rate constants with H_2O_2, the rate constants for Mn^{2+} were affected by the mutations.

Our results indicate that mutations in the axial ligand network have little if any effect on the reactivity of compound I or the ferric, resting enzyme. Our results indicate that the axial ligand environment only affects the reactions

of compound II and not those of compound I. This finding was predicted by the theoretical studies of Du and Loew (*28*). These workers performed a quantum chemical study using the "intermediate neglect of differential overlap" method to calculate the energy levels of various compound I complexes. The imidazole, imidazolate, acetylamide, phenolate, and thiolate ligands were used in the model. The imidazole and imidazolate models mimic the axial ligands of peroxidases where proton transfer to the nearby Asp residue imparts some basicity. The acetylamide model was chosen to mimic the fully active CcP mutant where the axial His is replaced by a Gln residue (*37*). The phenolate and thiolate ligands mimic the heme active sites of catalase and cytochrome P450. The effects of this wide range of axial ligands on the electron and spin distributions in the a_{1u} and a_{2u} radical cations of the compound I were moderate at best. These calculations are consistent with these results and the results of Sundaramoorthy (*37*) where changes in the network of axial ligands have little effect on compound I reactivity. For the D242 mutants and the F190 mutants, only one mutation, F190V, resulted in a decrease in the second-order rate constant of compound I with Mn^{2+}. Here, a 21% decrease in the rate constant was observed; however, this decrease had no consequence on the overall reactivity of the enzyme. The F190V mutation is the only one that caused an increase in k_{cat}. How MnP can generate a more reactive compound I, relative to other peroxidases, is not yet understood.

Mutations altering the reactivity of compound II would have a greater kinetic consequence because the reaction of compound II is the rate-limiting step in most if not all peroxidases (*11*, *38*, *39*). In MnP, the oxidation of Mn^{2+} by compound II follows a two-step process of an initial rapid equilibrium binding step followed by the oxidation of Mn^{2+} by the enzyme. None of the mutations caused a change in the binding of Mn^{2+}, although a decrease in the first-order rate constant of oxidation was observed. In the case of the D242S, F190L, F190V, and F190W mutants, this reduction in the rate of compound II reactions was sufficient to account for the decrease in steady-state activity; the rate of compound II reduction by chelated Mn^{2+} was $^1/_2$ of that of the k_{cat} of the mutant enzyme. However, in the case of the D242E mutant, the rate of compound II reduction is higher than the k_{cat} of the enzyme. Clearly, in this case there must be another step in the reaction cycle limiting the overall rate of the enzyme. The pre-steady-state parameters we were able to measure, however, give no indication of which step this might be. The new rate-limiting step of the reaction cycle could not involve the reaction of the ferric enzyme with H_2O_2, or the reaction of compound I with either Mn^{2+} or H_2O_2, as all these reactions were unaffected by the mutation. It is possible that a product release step, which is not monitored in the single-turnover experiments used to measure the pre-steady state, has become rate limiting.

Our results on the role of F190 are in contrast to those of Kishi et al. (*36*). First, they characterized four mutants at this site, F190Y, F190L, F190I, and F190A. Their research did not provide a function of F190 in MnP other than indicating that the F190 site may contribute to the overall stability of MnP, as well as to the stability of the heme environment of the enzyme. These workers showed that the F190I and F190A mutations were less stable than the wild-type enzyme, similar to the enzyme instability we found as a result of the F190W mutation. They were unable to express the F190W mutant. This was most likely the result of this instability. They used a homologous expression system that results in secreted active MnP holoenzyme, whereas we reconstituted active MnP from bacterially expressed inclusion bodies. This may account for our greater degree of success in generating the active, though unstable, F190W mutant. Kishi et al. (*36*) did not detect any changes in the steady-state kinetics of these mutants, except in the reactions of the F190A mutant with ferrocyanide. It is significant that, with the exception of the F190L mutant, we did not isolate any of these mutants in our activity screen. This would suggest that our screen for active mutants was not complete.

The finding that other mutants are active does not alter the interpretation of this study, that conclusion being that changes in the axial ligand network of MnP only alter the reactivity of compound II, not that of compound I. Unlike Kishi et al. (*36*), we found that the F190L mutation reduced the k_{cat} of MnP by 40%. Our results were confirmed by pre-steady-state kinetic analyses of the mutant, which revealed that the rate of reduction of F190L compound II by chelated Mn^{2+}, the rate-limiting step of the MnP catalytic cycle, was likewise reduced 40%. Kishi et al. (*36*) did not perform any pre-steady-state analyses on their mutants. The other F190 mutants generated for this study, F190V and F190W, also affected the steady-state and pre-steady-state kinetics of MnP. However, these mutant enzymes were not studied by Kishi et al. (*36*).

The results obtained here on the nature of compound I of the F190 mutant are in accord with Kishi et al. (*36*). These workers saw no evidence of a protein-centered radical in the compound I state of their F190Y mutant, just as we see no evidence of a protein-centered radical in the compound I state of the F190W mutant.

Similar mutations in the axial ligand network have been made in CcP. In CcP, D235, which serves the same role as D242 in MnP, has been mutated to E, Q, and A (*40*, *41*). Of these, only the D235E mutant of CcP retained significant steady-state activity (*41*). The D235Q mutant exhibited barely detectable activity (0.3% of the wild-type steady-state rate) (*42*). Similar to our findings, the D235Q mutation in CcP has a far less drastic effect on the reactions of CcP compound I than on the subsequent catalytic steps of that enzyme. The D235Q mutation does reduce the second-order rate constant for compound I formation in CcP, but only by 1 order of magnitude (*43*), whereas the steady-state rate of CcP catalysis was reduced by more than 2 orders of magnitude (*42*).

The D235E, D235Q, and D235A mutations in CcP are all thought to result in a weaker (or nonexistent, in the case of the D235A mutation) H bond being formed with the proximal His (*40*, *41*). These mutations raise the midpoint potential of the Fe^{3+}/Fe^{2+} couple of CcP (*41*). The midpoint potential of the Fe^{3+}/Fe^{2+} couple of heme peroxidases is thought in general to vary with the strength of the Asp$\cdots$His H bond at the proximal His, with stronger H bonds resulting in more negative midpoint potentials (*32*). The D235E mutation in CcP does not radically change the position of the carboxylate group that is interacting with the proximal His, despite resulting in a weaker H bond (*41*). In wild-type CcP, D235 forms a second H bond with W191, and the D235E mutant maintains this second H bond. As a

result of the D235E mutant of CcP retaining this H-bonding network, the helix bearing residue 235 in repositioned approximately 1 Å away from its wild-type position (*41*).

The F190 and D242 mutations in MnP also changed the midpoint potential of the Fe^{3+}/Fe^{2+} couple of the enzyme. This suggests that the electronic environment is influenced by both residues and that the kinetic alterations that arise in the mutants may be at least partly attributable to the perturbations in this environment. The F190L and F190W mutations, which decreased the activity of MnP, made the midpoint potential of the Fe^{3+}/Fe^{2+} couple more positive, while the F190V mutation, which increased the activity of MnP, made the midpoint potential more negative. The D242S and D242E mutations, which decreased the activity of MnP, appear to have made the midpoint potential of the Fe^{3+}/Fe^{2+} couple more negative. The F190 mutations affected the anodic and cathodic peaks of MnP about equally, which is consistent with the changes observed in the calculated midpoint potentials of these mutants. On the other hand, the D242 mutations affected the cathodic (oxidative) peaks of the CVs preferentially over the anodic (reductive) peaks. In this case, as the reduction of the Fe^{3+}/Fe^{2+} couple of MnP occurs much more readily than the oxidation, the lack of a shift in the anodic peaks of the D242E and D242S mutants suggests that changes to the midpoint potential of the Fe^{3+}/Fe^{2+} couple of these mutants might not be as large as the calculated value indicates. Nonetheless, the CVs of the D242 mutants are clearly altered from the wild-type MnP, suggesting that the electronic environment of the heme in these mutants has been perturbed, as it has been in the corresponding D245 mutants of CcP (*41*). Aside from assessing the electronic environment of the heme, we find it difficult to infer kinetic consequences from the results of the Fe^{3+}/Fe^{2+} couple. The heme iron during MnP catalysis actually cycles through Fe^{4+}/Fe^{3+} states. While changes in the midpoint potential of the Fe^{3+}/Fe^{2+} couple can be used to infer changes to the heme environment, they need not correlate exactly with changes to the catalytically relevant Fe^{4+}/Fe^{3+} couple. For instance, the reduction potential of the Fe^{3+}/Fe^{2+} couple in HRP isozyme C is 60 mV more negative than that of HRP isozyme A (*44*), but the reduction potential of the compound II/ferric enzyme (i.e., the Fe^{4+}/Fe^{3+}) couple of isozyme C is 80 mV more positive than that of isozyme A (*45*).

In CcP, the site equivalent to F190 in MnP is W191. A mutant CcP was generated where W191 was replaced by a Phe (*46*). Similar to results obtained here with MnP, the midpoint potential of the Fe^{3+}/Fe^{2+} couple is more positive with the Trp wild-type enzyme than the Phe-containing mutant enzyme. The W191F mutation in CcP also reduced the steady-state activity toward cytochrome c^{2+} 3000-fold. The detailed kinetic consequences of this mutation were not otherwise investigated. The D235E, D235N, and D235A mutations in CcP all raise the midpoint potential of the Fe^{3+}/Fe^{2+} couple of CcP (*41*).

In conclusion, our results on mutagenesis of D242 and F190 have shown that these residues affect the reactivity of the heme active site. The changes in the axial ligand H bonding network largely influence the reactivity of compound II (Fe^{4+}) and have little influence on the reactivity of compound I (porphyrin cation radical). Thus, the molecular basis for the highly reactive compound I of fungal peroxidases is yet to be determined.

REFERENCES

1. Buswell, J. A., and Odier, E. (1987) *Crit. Rev. Biotechnol. 6*, 1−60.
2. Cai, D., and Tien, M. (1993) *J. Biotechnol. 30*, 79−90.
3. Gold, M. H., and Alic, M. (1993) *Microbiol. Rev. 57*, 605−622.
4. Reddy, C. A., and D'Souza, T. M. (1994) *FEMS Microbiol. Rev. 13*, 137−152.
5. Kersten, P. J., Tien, M., Kalyanaraman, B., and Kirk, T. K. (1985) *J. Biol. Chem. 260*, 2609−2612.
6. Koduri, R. S., and Tien, M. (1995) *J. Biol. Chem. 270*, 22254−22258.
7. Glenn, J. K., Akileswaran, L., and Gold, M. H. (1986) *Arch. Biochem. Biophys. 251*, 688−696.
8. Waters, W. A., and Littler, J. S. (1965) in *Oxidation in Organic Chemistry* (Wiberg, K. B., Ed.) Vol. V, Academic Press, New York.
9. Zweig, A., Hodgson, W. G., and Jura, W. H. (1964) *J. Am. Chem. Soc. 86*, 4124−4129.
10. Wariishi, H., Akileswaran, L., and Gold, M. H. (1988) *Biochemistry 27*, 5365−5370.
11. Kuan, I., Johnson, K. A., and Tien, M. (1993) *J. Biol. Chem. 268*, 20064−20070.
12. Tien, M., Kirk, T. K., Bull, C., and Fee, J. A. (1986) *J. Biol. Chem. 261*, 1687−1693.
13. Tien, M., and Tu, C.-P. D. (1987) *Nature 326*, 520−523.
14. Pease, E. A., Andrawis, A., and Tien, M. (1989) *J. Biol. Chem. 264*, 13531−13535.
15. Pribnow, D., Mayfield, M. B., Nipper, V. J., Brown, J. A., and Gold, M. H. (1989) *J. Biol. Chem. 264*, 5036−3040.
16. Piontek, K., Glumoff, T., and Winterhalter, K. (1993) *FEBS Lett. 315*, 119−124.
17. Sundaramoorthy, M., Kishi, K., Gold, M. H., and Poulos, T. L. (1994) *J. Biol. Chem. 269*, 32759−32767.
18. Edwards, S. L., Raag, R., Wariishi, H., and Gold, M. H. (1993) *Proc. Natl. Acad. Sci. U.S.A. 90*, 750−754.
19. Bangcharoenpaurpong, O., Champion, P. M., Hall, K. S., and Hager, L. P. (1986) *Biochemistry 25*, 2374−2378.
20. Champion, P. M., Stallard, B. R., Wagner, G. C., and Gunsalus, I. C. (1982) *J. Am. Chem. Soc. 104*, 5469−5472.
21. Fita, I., and Rossman, M. G. (1985) *J. Mol. Biol. 185*, 21−37.
22. Patterson, W. R., and Poulos, T. L. (1995) *Biochemistry 34*, 4331−4341.
23. Edwards, S. L., Xuong, N. h., Hamlin, R. C., and Kraut, J. (1987) *Biochemistry 26*, 1503−1511.
24. Finzel, B. C., Poulos, T. L., and Kraut, J. (1984) *J. Biol. Chem. 259*, 13027−13036.
25. Kunishima, N., Fukuyama, K., Wakabayashi, S., Sumida, M., Takaya, M., Shibano, Y., Amachi, T., and Matsubara, H. (1993) *Proteins: Struct., Funct., Genet. 15*, 216−220.
26. Petersen, J. F. W., Kadziola, A., and Larsen, S. (1994) *FEBS Lett. 339*, 291−296.
27. Valentine, J. S., Sheridan, R. P., Allen, L. C., and Kahn, P. C. (1979) *Proc. Natl. Acad. Sci. U.S.A. 76*, 1009−1013.
28. Du, P., and Loew, G. H. (1992) *Int. J. Quantum Chem. 44*, 251−261.
29. Nelson, D. P., and Kiesow, L. A. (1972) *Anal. Biochem. 49*, 474−478.
30. Whitwam, R., and Tien, M. (1996) *Arch. Biochem. Biophys. 333*, 439−446.
31. Kunkel, T. A., Bebenek, K., and McClary, J. (1991) *Methods Enzymol. 204*, 125−139.
32. Millis, C. D., Cai, D., Stankovich, M. T., and Tien, M. (1989) *Biochemistry 28*, 8484−8489.
33. Cleland, W. W. (1983) in *Contemporary Enzyme Kinetics and Mechanism* (Purich, D. L., Ed.) Vol. II, pp 253−266, Academic Press, Orlando, FL.
34. Bard, A. J., and Faulkner, L. R. (1980) *Electrochemical Methods, Fundamentals and Applications*, Wiley, New York.
35. Kuan, I.-C., and Tien, M. (1993) *Proc. Natl. Acad. Sci. U.S.A. 90*, 1242−1246.

36. Kishi, K., Hildebrand, D. P., Someren, M. K.-v., Gettemy, J., Mauk, A. G., and Gold, M. H. (1997) *Biochemistry 36*, 4268−4277.
37. Sundaramoorthy, M., Chondhury, K., Edwards, S. L., and Poulos, T. L. (1991) *J. Am. Chem. Soc. 113*, 7755−7757.
38. Koduri, R. S., and Tien, M. (1994) *Biochemistry 33*, 4225−4230.
39. Hahm, S., Miller, M. A., Geren, L., Kraut, J., Durham, B., and Millett, F. (1994) *Biochemistry 33*, 1473−1480.
40. Wang, J. M., Mauro, M., Edwards, S. L., Oatley, S. J., Fishel, L. A., Ashford, V. A., Xuong, N. H., and Kraut, J. (1990) *Biochemistry 29*, 7160−7173.
41. Goodin, D. B., and McRee, D. E. (1993) *Biochemistry 32*, 3313−3324.
42. Ferrer, J. C., Turano, P., Banci, L., Bertini, I., Morris, I. K., Smith, K. M., Smith, M., and Mauk, A. G. (1994) *Biochemistry 33*, 7819−7829.
43. Vitello, L. B., Erman, J. E., Miller, M. A., Wang, J., and Kraut, J. (1993) *Biochemistry 32*, 9807−9818.
44. Yamada, H., Makino, R., and Yamazaki, I. (1975) *Arch. Biochem. Biophys. 169*, 344−353.
45. Hayashi, Y., and Yamazaki, I. (1979) *J. Biol. Chem. 254*, 9101−9106.
46. Mauro, J. M., Fishel, L. A., Hazzard, J. T., Meyer, T. E., Tolin, G., Cusanovich, M. A., and Kraut, J. (1988) *Biochemistry 27*, 6243−6256.

BI982568E